ISSN 1330-3651 (Print), ISSN1848-6339(Online) https://doi.org/10.17559/TV-20221109190210
Preliminary communication

Approximation of Electric Field in Biological Tissue

Vladimir STANKOVIĆ*, Dejan JOVANOVIĆ, Nenad CVETKOVIĆ, Milan BLAGOJEVIĆ, Miomir RAOS

Abstract: This paper presents the method of homogenization of several different biological tissues in order to simplify the numerical calculation of the electric field distribution in certain biological structures of interest. For this purpose, a 3D model was used with blocks that have the same electromagnetic characteristics as their corresponding biological tissues of the human head. The results obtained in the case of homogenized block model were compared with the ones obtained by using the original heterogeneous model containing the following tissues: skin, fat, muscle, bone, and brain. Homogenization of the model has been caried out only for the layers that precede the layer in which the analysis of electric field distribution was performed. A smart phone was used as the source of electromagnetic radiation at a frequency of 0,9 GHz. A comparative analysis of the electric field intensity in the layer of interest indicates good matches for the heterogeneous and homogenized models. Based on the obtained results, deviations in the electric field intensity can be observed for both models. These deviations range from 3,7% to 5,2% for different layer thicknesses.The proposed homogenization method significantly simplifies the modelling and also reduces the simulation time required to obtain appropriate results.

Keywords: biological tissue; electric field; mobile phone; numerical models

1 INTRODUCTION

If a biological tissue stands in the way of electromagnetic (EM) wave propagation, the wave will penetrate the tissue and a part of the wave energy will be absorbed by the tissue. When an electromagnetic wave passes from one biological medium to another, there is a difference between the input and the output wave energy at the separation surface. This difference represents the absorbed energy.

Calculation of an EM field inside a human body is very complex, because the human body is a heterogeneous, nonlinear, and dispersive medium. Therefore, it is necessary to use an adequate numerical method. Numerical calculations are a combination of mathematical methods and field theory and they require using a mathematical model to correctly describe the problem by means of differential equations, integral equations, or variance expressions [1-5].

The results presented in [1] showed that the modeling of electric field distribution in tissues during electroporation has to take into account the changes in electrical conductivity when an electroporation-based treatment is planned.

In study [3], the mathematical model of electromagnetic parameters devoted to Specific Absorption Rate (SAR) was developed using a Debye Model. An anthropomorphic phantom model for the SAR test was created based on the geometric parameters by following the principles of resemblance and consistent conductivity.

An analytical model for investigating the feasibility of sinusoidal transmission of an electric field across a frozen physiological layer into biological tissue is presented in [4]. The concept was analyzed for frequencies in the range of conventional electroporation frequencies and electric field intensity.

The authors of [5] used an improved Newton's method to predict pulse voltages and to verify the fit of the method for different tissue parameters in a numerical calculation developed for electroporation.

Study [6] describes some numerical methods developed for the calculation of induced electric fields and SAR in the case of anatomically based heterogeneous models of the human body. The impedance method used at lower frequencies and the finite difference time domain (FDTD) method, which can be used at any frequency of interest, are also presented.

The numerical methods for solving Maxwell's equations are presented in [7]. Numerical methods that describe the interactions of EM fields with the human body provide a way to obtain information that is necessary for assessing the exposure of biological tissues to EM fields.

A new methodology for empirical comparisons of competitive computational methods for solving bioelectromagnetic problems is presented in [8]. The methodology is tested by comparing three numerical methods for performing bioelectromagnetic simulations: Finite-Difference Time-Domain (FDTD) and two Fast Fourier Transform (FFT)-accelerated integral-equation methods, Adaptive Integral Method (AIM), and Generalized Minimal Residual variant (GMRES-FFT).

Numerical methods for solving electromagnetic field problems are presented in [9]. The purpose of numerical electromagnetics is to find solutions to Maxwell's equations or equations derived from them that satisfy all boundary conditions, electromagnetic properties of materials, as well as excitation conditions specific to a given problem.

Study [10] refers to an overview of Fractional Calculus (FC) methods in electromagnetic theory, as well as their application to dielectric relaxation modeling. Various numerical techniques related to the dispersive dielectric media are discussed through simulations based on FDTD methods.

The procedure for determination of the dielectric properties of heterogeneous materials that have complex permittivity parameters is considered in [11]. Several different accepted mixing rules are presented and the effects of structure and internal geometry of the mixture on the effective permittivity are illustrated.

In [12], the internal homogenization method is introduced to determine the effective physical properties (permittivity and conductivity) of biological tissues. This method is performed on a 2D child head model obtained from MRI data. The obtained results are compared with the results obtained from the original heterogeneous model and

effective medium theories such as Maxwell-Garnett and Polder van Santen.

Homogenization has an important role in simplifying the structure and reducing the time required for numerical calculation of EM field propagation in biological structures. Homogenization consists of replacing the entire complex structure with a simplified model that has effective physical properties. In some studies [10, 12, 13], different approaches to the homogenization procedure of the multilayer structure are proposed.

The new approach presented here is supposed to simplify the procedure of determining electric field distribution for a specific biological tissue. Specifically, if the goal is to determine electric field distribution in a tissue through which an EM wave propagates, having previously passed through another medium, then it is necessary to consider all parameters that may affect a change in the EM wave. The wave can be affected to a greater or lesser extent by the composition of the media through which it propagates, whether they are biological or other media, as well as by the conditions at the separation areas between two different media. This results in a change of electromagnetic wave penetrating depth or the energy carried by the wave.

This model is designed so that all the layers/media on the path of the electromagnetic wave to the certain biological tissue for which it is important to determine the electric field distribution can be approximated into a single layer.

2 ELECTROMAGNETIC PROPERTIES OF BIOLOGICAL TISSUES

Detailed knowledge of dielectric properties of biological tissues is essential to the understanding of interaction between EM radiation and the human body. EM properties of tissues, which are frequency dependent, are described using the dielectric constant ε magnetic permeability μ, and specific conductivity σ. These parameters describe the interaction of external EM field with biological tissue.

For almost all media, the values of EM parameters vary depending on the signal frequency.

Biological tissues can be viewed as materials whose relative magnetic permeability μ_r is presumed to be 1 and that $\mu = \mu_0$.

Dielectric properties of materials are determined by a complex relative dielectric constant $\underline{\varepsilon}_r$ [14], which is expressed as

$$\underline{\varepsilon}_r = \varepsilon_r' - j\,\varepsilon_r'' \tag{1}$$

where ε_r' is the real part of the relative dielectric constant and it denotes the charge displacement and, consequently, displacement of the energy present in the material; ε_r'' is the imaginary part of the relative dielectric constant, also called the external loss factor, and it denotes the power dissipation [14].

Conductivity is the result of free charge movement, while permittivity occurs due to stationary dipoles. In a stable state, the difference between conductivity and dielectric constant is clear, but at higher frequencies the two become connected.

The complex electrical conductivity $\underline{\sigma}$ [14] can be represented as

$$\varepsilon_r'' = \sigma / \omega\varepsilon_0 \tag{2}$$

where ω (rad/s) is the angular frequency ($\omega = 2\pi f$).

Both the real and the imaginary parts of complex conductivity may depend on the frequency.

For many bioelectric phenomena, the first expression in Eq. (2) is much larger than the second, so the tissue can be presented as purely conductive [15].

The external loss factor ε_r'' is connected with electrical conductivity via the following equation [14]:

$$\underline{\sigma} = \sigma + j\,\omega\varepsilon \tag{3}$$

where ε_0 is the dielectric constant of vacuum and ω is the angular frequency of the field.

Several techniques that provide a numerical solution to Maxwell's equations are available. They can generally be classified into two categories - those based on the differential equation (DE) and those based on the integral equation (IE). Further classification can be made according to whether the calculation is performed in the time domain or the frequency domain. Some of those methods include Finite-Difference Time Domain (FDTD), Finite Integration Technique (FIT), Method of Moments (MoM), and Finite-element Method (FEM) [7].

As stated, the electrical properties of tissue are frequency dependent and therefore dispersive. Consequently, the frequency dependence of ε and σ must be taken into account at high frequencies.

Dispersion can be represented using the Debye and Cole-Cole formulation [14, 16] in the form of equations:

$$\hat{\varepsilon}(\omega) = \varepsilon_\infty + \sum_n \frac{\Delta\varepsilon_n}{1 + (j\omega\tau_n)^{(1-\alpha_n)}} + \frac{\sigma_i}{j\omega\varepsilon_0} \tag{4}$$

where $\hat{\varepsilon}$ is the complex relative permittivity as a function of ω; ε_0 is the permittivity of free space; ε_∞ is the permittivity at frequencies for which $\omega\tau \gg 1$; $\Delta\varepsilon_n = \varepsilon_s - \varepsilon_\infty$ is the magnitude of the dispersion; ε_s is the permittivity when $\omega\tau \ll 1$; σ_i is static conductivity; and α_n is the contribution to the broadening of the dispersion.

In [17], the use of a multiple Debye parameterization of the form was proposed in order to optimize the time needed to perform calculations

$$\hat{\varepsilon}(\omega) = \varepsilon_\infty + \frac{\varepsilon_{s1} - \varepsilon_\infty}{1 + j\omega\tau_1} + \frac{\varepsilon_{s2} - \varepsilon_\infty}{1 + j\omega\tau_2} \tag{5}$$

Some studies present the concepts of dielectric mixing. Based on it, the effective permittivity of the mixture can be calculated as a function of the permittivity of the integral parts, their fractional volumes, and potentially of other parameters that characterize the microstructure of the mixture [11]. In [12], the possibility of modifying electrical

parameters in order to achieve homogenization of biological tissues is shown.

3 NUMERICAL MODELS

3.1 Electromagnetic Radiation Source

The source of radiation is represented by a numerical model of a smart phone [18-20] containing a casing, a display, and an antenna (Fig. 1).

Figure 1 Actual smart phone

The mobile phone antenna is a planar inverted F antenna (PIFA) with S-Parameter characteristic, as shown in Fig. 2. The operating frequency of mobile phone $f = 0{,}9$ GHz is used in this study while the output power is $P = 1$ W [21] and the impedance is $Z = 50\ \Omega$.

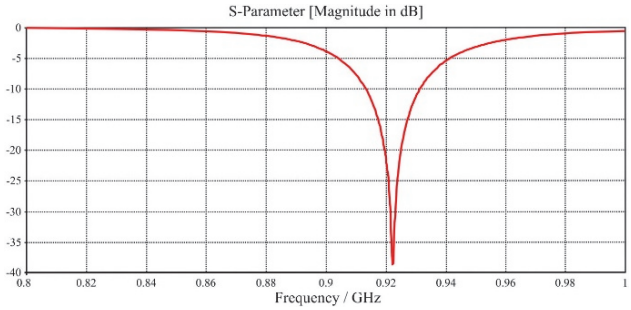

Figure 2 S-Parameter of the PIFA antenna for f =0,9 GHz

3.2 Numerical Block Models of Biological Tissue

The model for biological tissues was created as a block model in which each block represents one biological tissue (Fig. 3). The layout of biological tissues was selected so as to match the actual order of tissues and organs of the human head [18-20, 22-24]. The realistic layout of tissues and organs in a human head is shown in Fig. 4.

Colours on the left of Fig. 4 correspond to the colours of tissues/organs on the right. Comparison of obtained values of electric field distribution will be made along the horizontal blue line passing through the block model.

Each block is described according to the EM properties of the biological tissue it represents. Tab. 1 provides the EM properties of human head tissues/organs used in the simulations for the operating mobile phone frequency of 0,9 GHz [25].

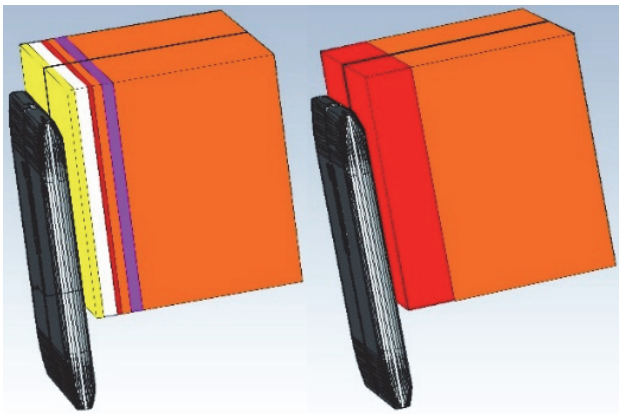

Figure 3 External appearance of the block model

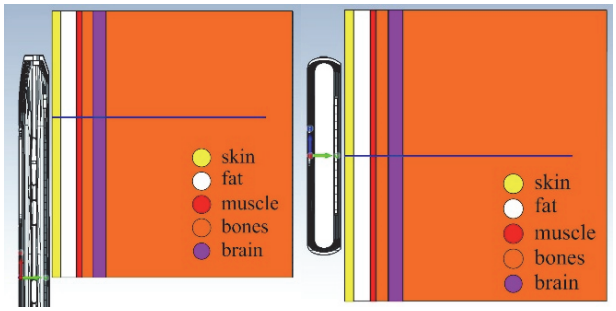

Figure 4 Vertical and horizontal cross-section of the model

The entire modelling of the mobile phone and the block model representing biological tissues, as well as the entire simulation of EM wave propagation from the mobile phone, were carried out using CST Studio Suite [26]. This software is based on the FIT (Finite Integration Technique) method [27].

The simulation yielded the EM field distribution inside the block model representing biological tissues. The values obtained for electric field intensity for different block types were used to verify the accuracy of the approximation method.

Table 1 Electromagnetic properties of tissues and organs at f = 0,9 GHz

Tissues	ε_r	σ / Sm^{-1}	ρ / kgm^{-3}
1. Skin	38,9	1,180	1109
2. Fat	11,0	0,190	911
3. Muscle	53,5	1,340	1090
4. Bones	11,8	0,275	1908
5. Brain*	46,1	1,710	1046

* Electromagnetic properties defined as average value

4 ELECTRIC FIELD IN BIOLOGICAL TISSUE

The following conditions apply for electric field components at the separation surface between the two media (Fig. 5):

$$E_{1t} = E_{2t} \tag{6}$$

$$\sigma_1 E_{1n} = \sigma_2 E_{2n} \tag{7}$$

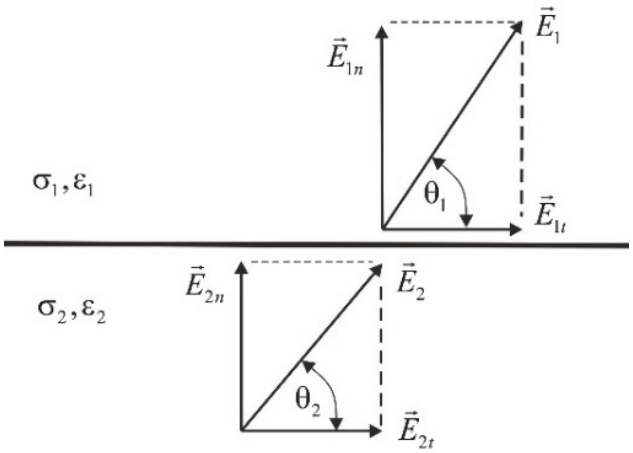

Figure 5 Components of electric field strength vector at the separation surface

When the surface charge density on the separation surface is equal to zero, applying appropriate mathematical transformations will yield the relation between the complex representatives of normal components of the electric field strength vector in both media [28]:

$$\underline{E}_{1n} = \frac{\sigma_2 + j\omega\varepsilon_2}{\sigma_1 + j\omega\varepsilon_1}\underline{E}_{2n} \tag{8}$$

Effective values can also be applied in the same way:

$$\left|\frac{\underline{E}_{1n}}{\underline{E}_{2n}}\right| = \left|\frac{\sigma_2 + j\omega\varepsilon_2}{\sigma_1 + j\omega\varepsilon_1}\right| \tag{9}$$

During propagation in a biological tissue, field strength and energy absorption are attenuated. The electric field amplitude will then change according to the following law:

$$E_2 = E_1 \, \mathrm{e}^{-\alpha z} \tag{10}$$

where E_2 is the field intensity at distance z from the separation surface, E_1 is the field intensity at the separation surface, and α is the attenuation constant

$$\alpha = \omega\sqrt{\frac{\varepsilon\,\mu}{2}\left(\sqrt{1+\frac{\sigma^2}{\omega^2\varepsilon^2}}-1\right)} \tag{11}$$

The attenuation constant is equal to the reciprocal value of penetration depth δ, which is determined as

$$\delta = \frac{1}{\omega}\left(\frac{\varepsilon\mu}{2}\left(\sqrt{1+\frac{\sigma^2}{\omega^2\varepsilon^2}}-1\right)\right)^{-\frac{1}{2}} \tag{12}$$

4.1 Averaging of Quantities

The approximation procedure, or the simplification of calculation, is shown in Fig. 6. Let us assume that we wish to qualify the electric field distribution in the nth medium. As the field distribution in the media preceding the target medium is not of interest at this point, it is necessary to simplify all calculations pertaining to these media as much as possible, while preserving a high degree of calculation accuracy.

The upper portion of Fig. 6 shows the entire series of different media (layers), described according to their EM properties. During the calculation, for each of these media, attention should be given exactly to the EM properties, to the thickness of the media/layers themselves, and to the conditions at the separation surface. All this complicates the entire calculation process and extends calculation time.

The same figure also shows how the approximation, i.e., simplification of the problem, was performed. Namely, all layers preceding the layer of interest were unified into a single layer, with an appropriate choice of parameters that describe the newly-formed layer. All the parameters describing this layer are the same as for every individual layer, the only difference being that averaging was applied. The EM parameter values of each individual medium were considered and an approximation was performed for each separate parameter. The averaging procedure is given by Eqs. (13) to (15).

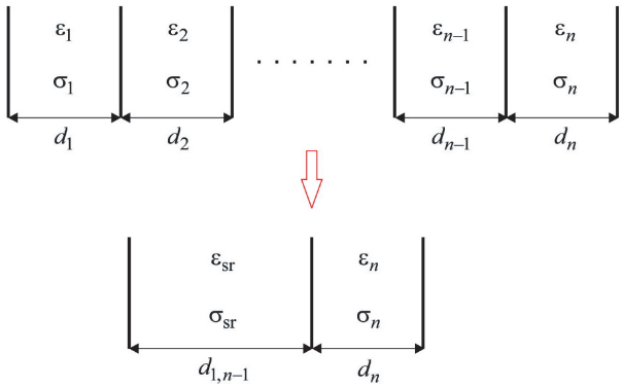

Figure 6 Procedure of averaging multiple layers into a single layer

The expressions for averaged ε, σ, and ρ are:

$$\varepsilon_{\mathrm{sr}} = \frac{\varepsilon_1 d_1 + \varepsilon_2 d_2 + \ldots + \varepsilon_{n-1} d_{n-1}}{d_1 + d_2 + \ldots + d_{n-1}} \tag{13}$$

$$\sigma_{\mathrm{sr}} = \frac{\sigma_1 d_1 + \sigma_2 d_2 + \ldots + \sigma_{n-1} d_{n-1}}{d_1 + d_2 + \ldots + d_{n-1}} \tag{14}$$

$$\rho_{\mathrm{sr}} = \frac{\rho_1 d_1 + \rho_2 d_2 + \ldots + \rho_{n-1} d_{n-1}}{d_1 + d_2 + \ldots + d_{n-1}} \tag{15}$$

5 RESULTS

The verification of the accuracy of the applied method will be analyzed for multiple different simulations of EM wave propagation from the mobile phone. To obtain results that are as accurate as possible, for every simulation, identical conditions were used for the phone radiation and for the entire space encompassed by the simulation.

Every simulation utilized a block model with identical external dimensions and with layers simulating specific biological tissues, as shown in Fig. 4. All tissues are described using their corresponding EM properties. The only difference between the blocks used in the simulation is the thickness of individual layers, which should

simultaneously serve as the indicator of potential application of approximation methods in the calculation of electric field distribution inside a specific biological tissue.

For every example, we created two numerical block models and two simulations of the effects of mobile phone radiation on the given models. The first block model contains all six layers (biological tissues), ordered as follows: the skin, fatty tissue, muscles, skull bones, the brain, and again skull bones.

In contrast, the second block model consists only of two layers. The first layer is a layer obtained through unifying the first five layers of the first block model into a single layer, while the second is identical to the sixth layer of the first block model. In the first layer of the second block model, we applied the previously described averaging of EM properties of all biological tissues constituting the layer.

5.1 Example I

Tab. 2 shows the thickness of every layer of the first block model viewed from the side of the mobile phone. Tab. 3 shows the EM properties of the averaged layer in the second block model, obtained by applying Eqs. (13) to (15).

Table 2 Dimensions of specific layers

Tissue	d / mm
Skin	2
Fat	2
Muscles	2
Bone	4
Brain	10

Table 3 EM properties of the averaged layer

EM properties
d = 20 mm
ε_r = 36,16
μ_r = 1
σ_r = 0,604 S/m
ρ_r = 1215,6 kg/m^3

Fig. 7 shows the electric field distribution for both block models. The electric field strength is limited to the same value in the colour palette for both cases, for improved visibility and comparability of field distribution in each individual layer.

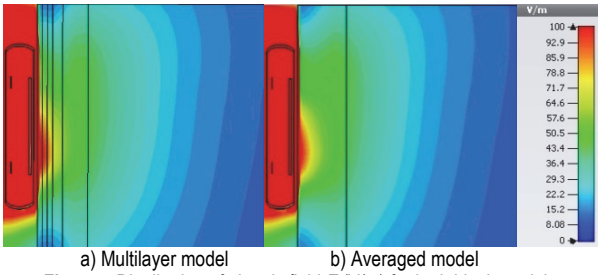

a) Multilayer model b) Averaged model

Figure 7 Distribution of electric field E (V/m) for both block models

As previously stated, the entire approximation model was conceived to produce the results of electric field distribution in a given biological tissue and to unify all the other tissues preceding it into a suitable single medium that will adequately represent them.

The distribution of the electric field for both models along the direction shown in Fig. 4 is represented in Fig. 8 and Fig. 9.

The distribution of the electric field along the layers that will be homogenized is shown in Fig. 8, while the distribution in the layer which is the same for both the homogeneous and the homogenized model and which starts 20 mm from the starting point is given in Fig. 9.

The graph shown in Fig. 9 indicates that the shape of the lines representing electric field intensity is the same after the 20 mm distance point for both models. Deviations in electric field intensity values are negligible, with 4,9% being the largest registered deviation for both models.

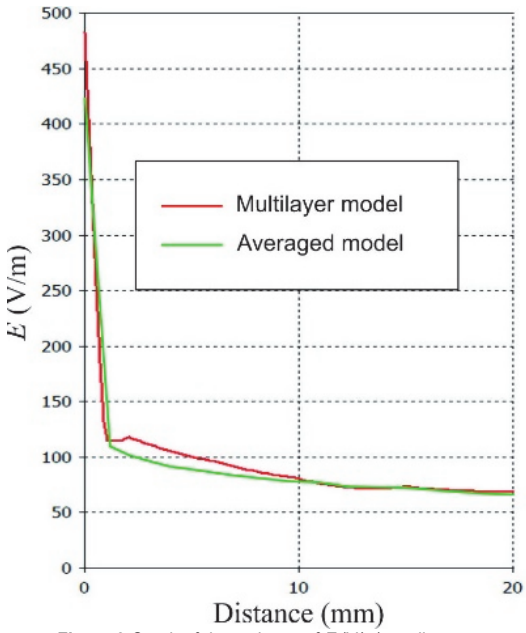

Figure 8 Graph of dependence of E (V/m) on distance

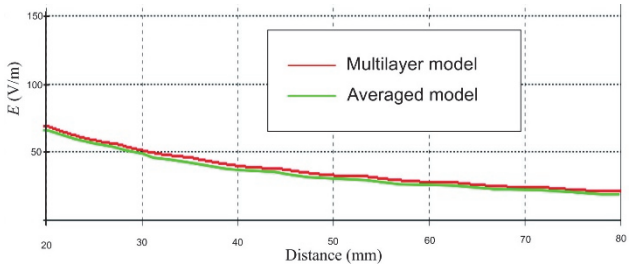

Figure 9 Graph of dependence of E (V/m) on distance

5.2 Example II

Tab. 4 and Tab. 5 show the thickness of layers in the first block model and the EM properties of the averaged layer in the second block model according to the same principle as in example I.

Table 4 Dimensions of specific layers

Tissue	d / mm
Skin	1
Fat	3
Muscles	5
Bone	6
Brain	5

Table 5 EM properties of the averaged layer

EM properties
d = 20 mm
ε_r = 32,7
μ_r = 1
σ_r = 0,53 S/m
ρ_r = 1298,5 kg/m^3

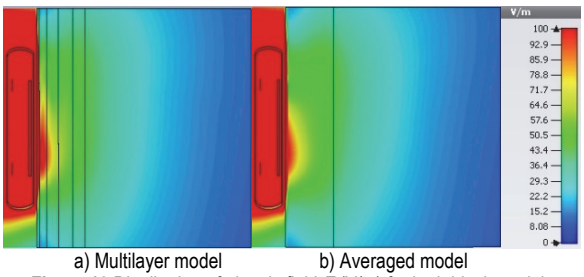

a) Multilayer model b) Averaged model

Figure 10 Distribution of electric field *E* (V/m) for both block models

The distribution of the electric field for both models along the direction shown in Fig. 4 is represented in Fig. 11 and Fig. 12.

As in the previous example, the averaged layer thickness is also 20 mm, so, the graph of electric field distribution after the 20 mm point is represented in Fig. 12.

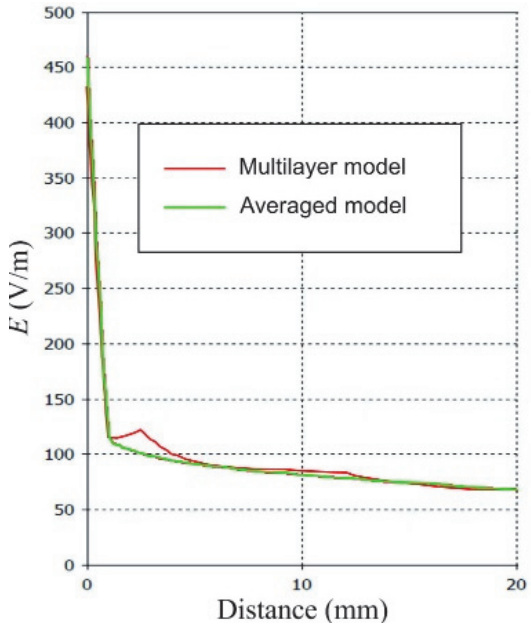

Figure 11 Graph of dependence of *E* (V/m) on distance

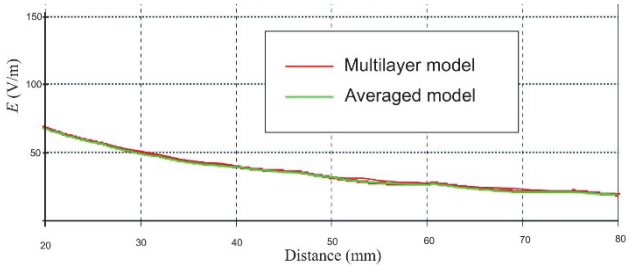

Figure 12 Graph of dependence of *E* (V/m) on distance

Line shapes indicate that electric field intensity values are approximately the same for both models, with 5,2% being the largest deviation of this value for the defined block models (Tab. 4 and Tab. 5).

5.3 Example III

Tab. 6 and Tab.7 show the thickness of layers in the first block model and the EM properties of the averaged layer in the second block model according to the same principle as in the previous two examples.

Table 6 Dimensions of specific layers

Tissue	*d* / mm
Skin	2
Fat	6
Muscles	2
Bone	4
Brain	6

Table 7 EM properties of the averaged layer

EM properties
$d = 20$ mm
$\varepsilon_r = 29{,}04$
$\mu_r = 1$
$\sigma_r = 0{,}477$ S/m
$\rho_r = 1191{,}75$ kg/m^3

Fig. 13 shows the electric field distribution for both block models defined according to the values given in Tab. 6 and Tab. 7, indicating that the electric field distribution in the last layer has approximately the same shape and value in both models.

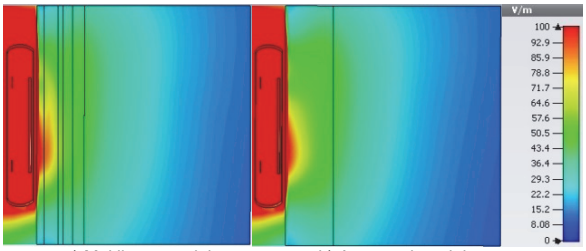

a) Multilayer model b) Averaged model

Figure 13 Distribution of electric field *E* (V/m) for both block models

The distribution of the electric field for both models along the direction shown in Fig. 4 is represented in Fig. 14 and Fig. 15.

The total thickness of the first five layers in the first model is 20 mm, so the thickness of the layer in the second model, which simulates the five layers, will also be 20 mm. Therefore, as in the previous examples, the analysis will be performed only after the 20 mm point in the graph (Fig. 15).

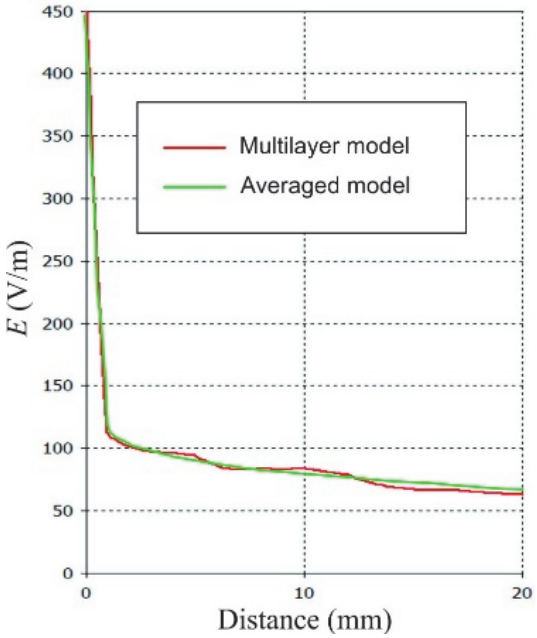

Figure 14 Graph of dependence of *E* (V/m) on distance

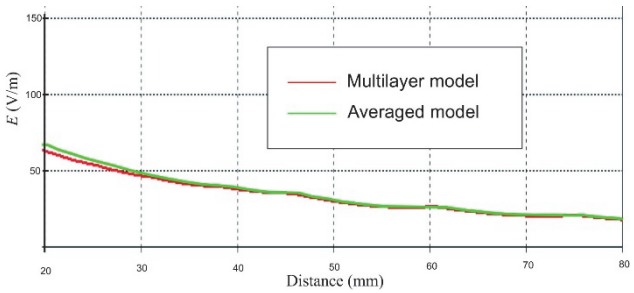

Figure 15 Graph of dependence of *E* (V/m) on distance

There is a noticeable overlap of the two lines representing electric field intensity along nearly the entire length of the same direction. In this example, the largest registered deviation of electric field intensity values in the two models is 3,7%.

6 CONCLUSION

The presented analyses of electric field intensity values in the nth layer indicate that the curves in all of the examples are of the same or very similar shape.

There are slight deviations in electric field intensity values at the separation surface of the nth layer, where the previous layer(s) is analyzed for comparison. There are also certain differences in field distribution through individual layers compared to the unified layer simulating them, but they are not of particular interest for the present analysis, because the presented approximation model is primarily designed to facilitate the calculation and analysis of field values in the layer of interest (biological tissue) rather than in all the other layers.

Through simulations of electromagnetic wave propagation, a block model consisting of several layers was considered. These layers represent the biological tissues described by their electromagnetic characteristics. For all three cases, it was of interest to determine the distribution of the electric field intensity in the last layer/tissue of the block models.

In case of solving a heterogeneous model, during the analysis, the influence of each layer/tissue on the electromagnetic wave propagation, must be taken into account, as well as the conditions at the separation surface of the two layers/tissues. Due to it, the approach of homogenization of multiple layers/tissues into one single layer was applied. The goal of this approach is that the propagation of the electromagnetic wave to the last layer of the model that is analyzed in detail should be as close as possible to the wave propagation in the case of a heterogeneous model. This has been shown to be possible if the homogenized layer adequately presents the layers/tissues it replaces.

The approximation procedure was applied to block models containing six layers of different thicknesses. The sixth layer is the layer of interest in which the distribution of electric field intensity is observed. Homogenized models consist of two layers, the first, which replaces the first five layers of the heterogeneous model, and the second, which is identical to the sixth layer of the heterogeneous model.

The agreement of the electric field intensity distribution for heterogeneous and homogenized models is analyzed in the last layers. The thickness of the homogenized layers is the same for all three models and is 20 mm. Consequently, the emphasis of the graphic comparison of the dependence of the electric field intensity as a function of distance is precisely from this distance to the end of the model.

In all simulations, it was shown that there is a very good agreement between the graphs of the heterogeneous and homogenized models, both in terms of shape and values. Deviations in the electric field intensity values are insignificant. For the first model, the maximum deviation is 4,9%, for the second, approximately the same, 5,2%, while for the third model, this deviation is the smallest and amounts to 3,7%.

These deviations of field values are chiefly the result of different thicknesses of individual layers that are simulated by the unified layer, because that component is the integral part of the expressions used to average the EM properties of certain media.

It was shown that, at the used frequency, a complex multilayer structure can be homogenized and replaced by a single layer and that the homogenization process does not affect the accuracy of the results, obtained in the case of a multilayer structure.

This method of homogenization greatly simplifies the modelling of the complex structure of the model by removing the boundaries between tissues and replacing their electromagnetic characteristics with homogeneous effective characteristics. Also, simulation with a partially homogeneous model is faster than one with a heterogeneous model.

Summarizing the obtained results for the electric field distribution, it can be concluded that this approach can be successfully used to estimate the distribution of the electric field in biological structure of interest since it reduces the entire calculation process as well as the simulation time.

In addition to the good agreement of the obtained results, there is still a small difference in the values of electric field, which can lead to potential instability of the system. The impact of this potential instability and its eventual detection and removal will be the subject of further research by the authors.

The proposed homogenization approach can have several advantages. First of all, the time required for the analysis of the EM wave propagation process as well as the use of computer hardware resources is significantly reduced. Significant savings in calculation time and computer resources can result in some optimization of software packages used for the analysis of EM wave propagation problems. Also, the process of creating models used in simulations can be faster and simpler, because their complexity is significantly reduced without losing the accuracy of the obtained results.

The homogenization approach could also be used to improve the actual phantom models used in laboratory conditions to measure the impact of mobile phones. Namely, these phantoms consist of two layers, a shell made of fiberglass and a fluid that represents the human brain with its EM properties. Replacing the fiberglass layer, with a layer whose EM characteristics will be obtained by the process of homogenization of the biological tissues it replaces, would result in more realistic values of the electric field in the fluid with the EM characteristics of the human brain.

Acknowledgements

This research was supported by the Ministry of Education, Science and Technological Development of the Republic of Serbia.

7 REFERENCES

[1] Corovic, S., Lackovic, I., Sustaric, P., Sustar, T., Rodic, T., & Miklavcic, D. (2013). Modeling of electric field distribution in tissues during electroporation. *BioMedical Engineering OnLine*, *12*(16). https://doi.org/10.1186/1475-925X-12-16

[2] Acosta, J. C. (2015). Electric fields and biological cells: numerical insight into possible interaction mechanisms.

[3] Li, S., Su, Z., Wang, H., Wang, Q., &Ren, H. (2018). Research on an Anthropomorphic Phantom for Evaluation of the Medical Device Electromagnetic Field Exposure SAR. *Applied Sciences*, *8*(10), 1929. https://doi.org/10.3390/app8101929

[4] Xiao, C. & Rubinsky, B. (2014). Theoretical analysis of AC electric field transmission into biological tissue through frozen saline for electroporation. *Bioelectromagnetics*, *35*, 607-613. https://doi.org/10.1002/bem.21881

[5] Xu, X., Yi, Z., &Yang, L. (2021). Numerical calculation for effectively simulating the electric field in electroporated tissue. *Journal of Physics: Conference Series*, 1861. https://doi.org/10.1088/1742-6596/1861/1/012101

[6] Gandhi, O. P. (1995). Some numerical methods for dosimetry: Extremely low frequencies to microwave frequencies. *Radio Science*, *30*(1), 161-177. https://doi.org/10.1029/94RS01158

[7] Hand, J. W. (2008). Modelling the interaction of electromagnetic fields (10 MHz - 10 GHz) with the human body: methods and applications. *Physics in Medicine and Biology*, *53*(16), 243-286. https://doi.org/10.1088/0031-9155/53/16/R01

[8] Massey, J. W., Wei, F., Geyik, C. S., & Yılmaz, A. E. (2018). A Methodology to Empirically Compare Computational Bioelectromagnetics Methods: Evaluation of Three Competitive Methods. *IEEE Transactions on Antennas and Propagation*, *66*(8), 4123-4136. https://doi.org/10.1109/TAP.2018.2835512

[9] Chen, Z., Wang, C. F. W., & Hoefer, J. R. (2022). A Unified View of Computational Electromagnetics. *IEEE Transactions on Microwave Theory and Techniques*, *70*(2), 955-969. https://doi.org/10.1109/TMTT.2021.3138911

[10] Mescia, L., Bia, P., & Caratelli, D. (2022). FDTD-Based Electromagnetic Modeling of Dielectric Materials with Fractional Dispersive Response. *Electronics*, *11*(10), 1588. https://doi.org/10.3390/electronics11101588

[11] Sihvola, A. (2000). Mixing Rules with Complex Dielectric Coefficients. *Subsurface Sensing Technologies and Applications*, *1*(4), 393-415. https://doi.org/10.1023/A:1026511515005

[12] Acikgoz, H. (2016). Internal Homogenization of Biological Tissues for Electromagnetic Dosimetry. *ACES Journal*, *31*(6), 706-711.

[13] Silly-Carette, J., Lautru, D., Gati, A., Wong, M. F., Wiart, J., & Fouad Hanna, V. (2008). Optimisation of the homogenization of tissues using the adjoint method and the FDTD. *International Microwave Symposium Digest, IEEE MTT-S*, 1361-1364. https://doi.org/10.1109/MWSYM.2008.4633030

[14] Miklavcic, D., Pavselj, N., & Hart, F. X. (2006). *Electric properties of tissues*, Wiley encyclopedia of biomedical engineering, *209*(922834401), 1-12. https://doi.org/10.1002/9780471740360.ebs0403

[15] Roth, B. J. (2006). *The Electrical Conductivity of Tissues*. The Biomedical Engineering Handbook: Second Edition. CRC Press.

[16] Gabriel, S., Lau, R. W., & Gabriel, C. (1996). The dielectric properties of biological tissues: III. Parametric models for the dielectric spectrum of tissues. *Physics in Medicine & Biology - IOPscience*, *41*(11), 2271-2293.

[17] Simicevic, N. (2005). Three-dimensional FDTD simulation of biomaterial exposure to electromagnetic nanopulses. *Phys.Med. Biol.*, *50*(21), 5041-53. https://doi.org/10.1088/0031-9155/50/21/007

[18] Stanković, V., Jovanović, D., Krstić, D., Marković, V., & Cvetković, N. (2017). Temperature distribution and specific absorption rate inside a child's head. *International Journal of Heat and Mass Transfer*, *104*, 559-565. https://doi.org/10.1016/j.ijheatmasstransfer.2016.08.094

[19] Stanković, V., Jovanović, D., Krstić, D., Marković, V., & Dunjić, M. (2017). Calculation of Electromagnetic Field from Mobile Phone Induced in the Pituitary Gland of Children Head Model. *Military Medical and Pharmaceutical Journal of Serbia*, *74*(9), 854-861. https://doi.org/10.2298/VSP151130279S

[20] Jovanovic, D. B., Stankovic, V., Cvetkovic, N. N., Krstic, D., & Vuckovic, D. (2019). The impact of human age on the amount of absorbed energy from mobile phone. *COMPEL*, *38*(5), 1465-1479.

[21] C95.3-2002 - IEEE Recommended Practice for Measurements and Computations of Radio Frequency Electromagnetic Fields with Respect to Human Exposure to Such Fields, 100 kHz - 300 GHz. https://doi.org/10.1109/IEEESTD.2002.94226

[22] Stanković, V., Marković, V., Jovanović, D., Krstić, D., & Cvetković, N. (2019). Distribution of the Absorbed Mobile Phone Energy at 1.8 and 2.1 GHz in a Child Head Model. *8th IEEE International Conference EUROCON*. https://doi.org/10.1109/EUROCON.2019.8861511

[23] Stanković, V., Jovanović, D., Marković, V., Krstić, D., & Cvetković, N. (2019). Distribution of the Magnetic Field from a Mobile Phone at 1.8 and 2.1 GHz through a Child Head Model. *14th International Conference TELSIKS 2019*, 121-124. https://doi.org/10.1109/TELSIKS46999.2019.9002143

[24] Stanković, V., Jovanović, D., Krstić, D., Zigar, D., & Malenović-Nikolić, J. (2020). Distribution of The Magnetic Field from a Mobile Phone at 0.9, 1.8 and 2.1 GHz Through a Child Head Model. *Safety Engineering*, *10*(2), 81-84. https://doi.org/10.5937/SE2002081S

[25] See http://www.itis.ethz.ch/itis-for-health/tissue-properties/database/dielectric-properties/

[26] See www.cst.com.

[27] Clemens, M. & Weiland, T. (2001). Discrete Electromagnetism with the Finite Integration Technique. *Progress in Electromagnetics Research*, *32*, 65-87. https://doi.org/10.2528/PIER00080103

[28] Barnes, F. & Greenebaum, B. (2007). *Handbook of Biological Effects of Electromagnetic Fields. Bioengineering and Biophysical Aspects of Electromagnetic Fields*. III ed., CRC Press.

Contact information:

Vladimir STANKOVIĆ, PhD, Assistant Professor
(Corresponding author)
University of Niš, Faculty of Occupational Safety,
Čarnojevića 10a, 18000 Niš, Serbia
E-mail: vladimir.stankovic@znrfak.ni.ac.rs

Dejan JOVANOVIĆ, PhD, Teaching Assistant
University of Niš, Faculty of Electronic Engineering,
A. Medvedeva 14, 18000 Niš, Serbia
E-mail: dejan.jovanovic@elfak.ni.ac.rs

Nenad CVETKOVIĆ, PhD, Associate Professor
University of Niš, Faculty of Electronic Engineering,
A. Medvedeva 14, 18000 Niš, Serbia
E-mail: nenad.cvetkovic@elfak.ni.ac.rs

Milan BLAGOJEVIĆ, PhD, Full Professor
University of Niš, Faculty of Occupational Safety,
Čarnojevića 10a, 18000 Niš, Serbia
E-mail: milan.blagojevic@znrfak.ni.ac.rs

Miomir RAOS, PhD, Full Professor
University of Niš, Faculty of Occupational Safety,
Čarnojevića 10a, 18000 Niš, Serbia
E-mail: miomir.raos@znrfak.ni.ac.rs